ANTIOXIDANTS & REDOX SIGNALING
Volume 23, Number 15, 2015

DOI: 10.1089/ars.2014.6139

Discoveries

ORIGINAL RESEARCH COMMUNICATION

# Specific Mechanisms Underlying Right Heart Failure: The Missing Upregulation of Superoxide Dismutase-2 and Its Decisive Role in Antioxidative Defense

Rolf Schreckenberg,[1] Manuel Rebelo,[1] Alexander Deten,[2] Martin Weber,[1] Susanne Rohrbach,[1] Márton Pipicz,[3,4] Csaba Csonka,[3,4] Péter Ferdinandy,[3,5] Rainer Schulz,[1] and Klaus-Dieter Schlüter[1]



## Abstract

***Aims:*** Research into right ventricular (RV) physiology and identification of pathomechanisms underlying RV failure have been neglected for many years, because function of the RV is often considered less important for overall hemodynamics and maintenance of blood circulation. In view of this, this study focuses on identifying specific adaptive mechanisms of the RV and left ventricle (LV) during a state of chronic nitric oxide (NO) deficiency, one of the main causes of cardiac failure. NO deficiency was induced in rats by L-NAME feeding over a 4 week period. The cardiac remodeling was then characterized separately for the RV/LV using quantitative real-time polymerase chain reaction, histology, and functional measurements. ***Results:*** Only the RV underwent remodeling that corresponded morphologically and functionally with the pattern of dilated cardiomyopathy. Symptoms in the LV were subtle and consisted primarily of moderate hypertrophy. A massive increase in reactive oxygen species (ROS) (+4.5 ± 0.8-fold, *vs.* control) and a higher degree of oxidized tropomyosin (+46% ± 4% *vs*. control) and peroxynitrite (+32% ± 2% *vs*. control) could be identified as the cause of both RV fibrosis and contractile dysfunction. The expression of superoxide dismutase-2 was specifically increased in the LV by 51% ± 3% and prevented the ROS increase and the corresponding structural and functional remodeling. ***Innovation:*** This study identified the inability of the RV to increase its antioxidant capacity as an important risk factor for developing RV failure. ***Conclusion:*** Unlike the LV, the RV did not display the necessary adaptive mechanisms to cope with increased oxidative stress during a state of chronic NO deficiency. *Antioxid. Redox Signal.* 23, 1220–1232.

## Introduction

FOR A LONG TIME, the right ventricle (RV) was viewed to play a marginal role in the maintenance and stability of global hemodynamics of adults. As a consequence, research into RV physiology, including the identification of specific pathomechanisms, has been a neglected subject of study, and only a few randomized clinical trials on RV failure have been carried out (29).

In this way, the range of therapeutic interventions available for RV failure corresponds largely to those for left ventricular (LV) failure. These interventions primarily target vasodilatation and thus at reducing cardiac afterload (34). However, the National Heart, Lung, and Blood Institute described the situation in a special report on the RV as follows: ''… right ventricular failure cannot be understood simply by extrapolating data and experience from left ventricular failure…The right ventricle is different from the left ventricle''(50).

The inadequate understanding of the RV pathophysiology, however, stands in sharp contrast to the frequency of RV failure, which does not differ from that of LV failure. The results of the CORE trial have also demonstrated that isolated RV failure or involvement of the RV in the cardiac symptoms

[1]Physiologisches Institut, Justus-Liebig-Universität Gießen, Giessen, Germany.
[2]Fraunhofer-Institut für Zelltherapie und Immunologie, Leipzig, Germany.
[3]Pharmahungary Group, Szeged, Hungary.
[4]Cardiovascular Research Group, Department of Biochemistry, University of Szeged, Szeged, Hungary.
[5]Department of Pharmacology and Pharmacotherapy, Semmelweis University, Budapest, Hungary.

**Innovation**

The results of the study demonstrate the inability of the right ventricular (RV) to cope with oxidative stress caused by a chronic deficiency in nitric oxide. The limited potential of the RV to increase its endogenous antioxidive capacity must be taken into consideration during the targeted development of new treatment stategies for RV insufficiency. The central role of the RV and its frequent involvement in numerous cardiovascular conditions underscore the necessity of viewing the RV pathophysiology as an independent entity, as it cannot simply be deduced from observations of the left ventricle.

is associated with a poorer prognosis compared with purely LV dysfunction (35).

However, the well-documented molecular and cellular mechanisms identified in the LV cannot readily be translated to the right heart. This situation can be substantiated by the specific cardiogenesis of the RV, the cellular origin of which can be traced back to the secondary or anterior heart field along with the septum and the outflow tract. In contrast, the atria and the entire LV originate from a population of progenitor cells that formed the primary heart field (49, 51).

At a molecular and cellular level, the pathogenesis and progression of chronic cardiac insufficiency can often be attributed to a reduced bioavailability of nitric oxide (NO), increased radical stress, and cardiac fibrosis (13, 27, 31).

In particular, the increased rate of cardiovascular events associated with chronic kidney diseases, type 2 diabetes mellitus, or women after menopause is ascribed to a general deficit of NO, among other factors (7, 48).

The effects of NO within the cardiovascular system are not solely attributed to its vasodilatory and thus antihypertensive properties. NO interacts far more ubiquitously at cellular and subcellular levels, in part, by nitrosation of cystein residues within signaling pathways of the renin-angiotensin-aldosterone system (RAAS), the sympathetic nervous system, and the mitochondria, and thus directly and indirectly influences the function and structure of the myocardium (21, 39, 45).

The primary research aim of this study is to identify the key enzymes and pathomechanisms that are specific and are regulated differently for the RV and LV during a state of systemic NO deficiency.

Chronic NO deficiency was induced in this study in female adult rats by feeding them the NOS inhibitor L-NAME over a period of 4 weeks. The effects of reduced NO levels on molecular and cellular parameters were studied for both ventricles.

During long-term application of L-NAME, the symptoms in experimental animals could only, in part, be attributed to the immediate reduction in the NO-dependent effects. Over the further course, a chronic deficiency in NO led to increased formation of reactive oxygen species (ROS) that not only favor the development of hypertension but also directly affect cell and organ functions. For this reason, the pure L-NAME substitution was supplemented by two additional applications. One treatment group also received the angiotensin-converting enzyme (ACE)-inhibitor captopril, while another was given the radical scavenger and superoxide dismutase (SOD)-mimetic tempol in the form of a therapeutic intervention in the third and fourth week of L-NAME application. Along with its interaction with the RAAS and the subsequent reduction in angiotensin-II-dependent effects, captopril also has direct antioxidant properties *via* a cleavable sulfhydryl group (36). The use of tempol allowed the identification of protective effects that can be attributed solely to a reduction in ROS.

Signal mechanisms and their effect on the contractile behavior after chronic exposure to L-NAME were also analyzed *in vitro* in cardiomyocytes isolated from the RV or LV independent of systemic influences and blood pressure.

## Results

### *Effect of L-NAME on systemic hemodynamics*

The systolic blood pressure averaged $126 \pm 7$ mm Hg with no group differences between all test groups at the start of the experimental protocol. This value did not change throughout the entire course of the experiment for the animals in the control group. In the L-NAME group (L), systolic blood pressure increased to $173 \pm 7$ mm Hg after 4 weeks. On addition of the ACE-inhibitor captopril to the L-NAME feed after 2 weeks of treatment (LC) for the remaining 2 weeks, the blood pressure fell from $159 \pm 5$ mm Hg (after 2 weeks of L-NAME) to $135 \pm 5$ mm Hg at 4 weeks. The supplemental application of the SOD-mimetic tempol (LT) did not result in a fall in blood pressure but prevented a further increase during the last 2 weeks of the treatment period ($161 \pm 4$ mm Hg). The heart rate did not change significantly in the entire collective throughout the observation period (Supplementary Fig. S1 and Supplementary Table S1; Supplementary Data are available online at www.liebertpub.com/ars).

### *Consequences of chronic NO deficiency on the cardiac remodeling*

The wet weights of the RV and LV were standardized to the body weight (BW) of the particular animal. Compared with the control group, the animals in the L and LT groups developed low-grade LV hypertrophy based on a moderate increase in the LV/BW ratio. Captopril normalized the ratio to the level of the control animals (Fig. 1A).

No significant difference could be detected compared with the drinking-water controls for the RV/BW ratio independent of the particular application scheme (Fig. 1A).

The raw data obtained for BW, the RV and LV, and lungs and kidneys are listed in Supplementary Table S2.

However, the geometry of the RV changed in L-NAME-fed animals and corresponded to the clinical picture of dilated cardiomyopathy. The supplemental application of captopril or tempol was able to positively affect the structural remodeling of the RV—the RV dilatation was reduced, and the decrease in the wall thickness was almost prevented (Fig. 1B, C).

On a molecular level, the remodeling of the RV and LV was characterized by re-expression of fetal genes. Brain natriuretic peptide and myosin heavy-chain beta were induced to a comparable level by L-NAME in both the RV and the LV. The induction of atrial natriuretic peptide (ANP), which is primarily re-expressed in response to cardiac pressure load, was increased only in the LV by $7.8 \pm 1.3$ fold (Supplementary Fig. S2).

### *Functional consequences of the structural remodeling*

The consequences of the L-NAME-induced remodeling on cardiac function were analyzed at the end of the 4-week

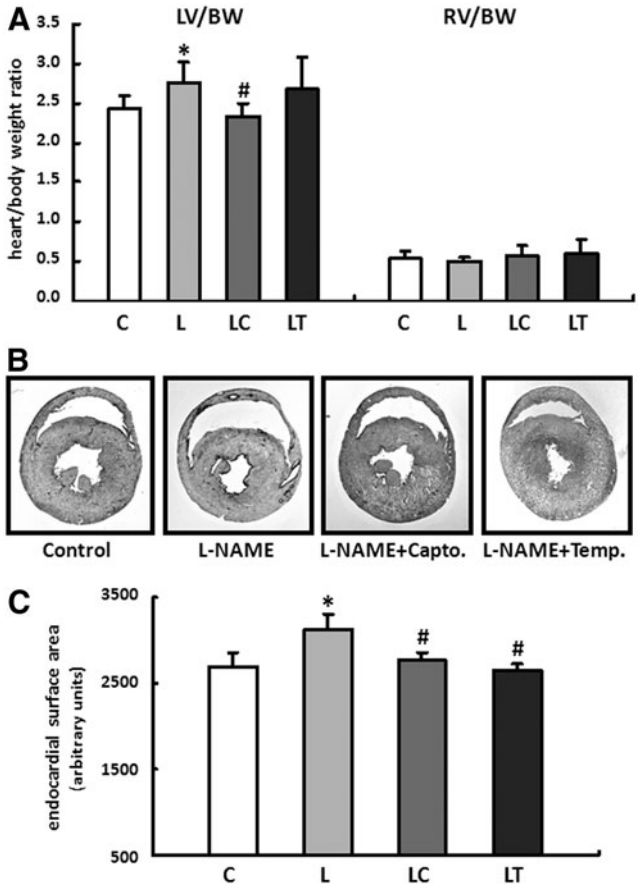


**FIG. 1. L-NAME induced changes in cardiac remodeling. (A)** Effects of the different treatment strategies on myocardial hypertrophy. The wet weight of the right ventricle (RV) and left ventricle (LV) were normalized to the body weight (BW) of the particular animal. Data are means ± S.D. of $n = 8$ hearts. **(B)** Representative images of horizontal heart sections from each treatment group. The geometry of the RV changed in L-NAME fed animals and corresponded with the pattern of dilated cardiomyopathy. **(C)** Endocardial surface area of the RV was determined from histological sections. Data are means ± SD of $n = 5$ hearts. $^{*}p < 0.05$ *versus* control, $^{\#}p < 0.05$ *versus* L-NAME.

substitution using a Millar tip catheter that was advanced on the right side to the RV *via* the jugular vein and atrium. The stabilized signal was then recorded continuously over a period of 30 min.

The peak RV pressure was reduced as a result of the L-NAME application and was affected only by captopril treatment. However, both therapy strategies significantly improved the RV dp/dt max or RV dp/dt min and thus specifically reduced the contractile dysfunction of the RV (Table 1).

As the cardinal symptom of impaired RV function, the blood accumulation was determined using the liver wet weight (LW) and the liver transaminases glutamate-oxaloacetate transaminase/glutamate-pyruvate transaminase (GOT/GPT). In animals fed L-NAME, the LW/BW ratio increased by 9.2% ± 0.6% (C *vs.* L, 29.4 g/kg *vs.* 32.1 g/kg, $p = 0.10$) while the transaminases rose by 14.8% ± 1.7% (C *vs.* L, 85.8 U/L *vs.* 98.4 U/L, $p = 0.01$).

The LV function, represented by the LV-developed pressure (LVDP), was determined using a balloon catheter. Regardless of the particular application scheme, no significant differences in the LVDP, the LV dp/dt max, or LV dp/dt min could be detected (Supplementary Table S3). Uniform lung wet weights largely rule out a restrictive functional disorder (Supplementary Table S2).

### *Regulation of the ROS in the right and left ventricles*

As previously stated in the introduction, chronic deficiency in NO is often associated with an increase in oxidative stress.

The fluorescence microscopy images of the dihydroethidium (DHE) staining showed only a slight radical load for the LV independent of the particular application scheme with no significant differences between the treatment groups.

In contrast to this, the RV had an elevated radical load even in untreated controls compared with the LV, and this was further increased till 4.5 ± 0.8-fold during L-NAME substitution. The two therapy options, captopril and tempol, significantly reduced the concentration of ROS in the RV to a comparable level (Fig. 2A, B).

It could already be seen that an increased accumulation of ROS contributes to contractile dysfunction by oxidative modification of tropomyosin (Tm) (14, 15). The formation of disulphide cross-bridges (DCB) at the level of cystein residues leads to an enhanced dimerization of Tm, which could be detected as high-molecular-weight peptide (~80 kDa) under non-reducing conditions in immunoelectrophoresis. L-NAME application did not have any effects on DCB formation in the LV; however, in the RV, a significant increase in cross-linking processes was detected, leading to a 46% ± 4% increase in oxTm/Tm ratio (Fig. 3A, B).

Given the specific changes in oxidative stress measured by DHE staining, a specific powerful oxidant species, peroxynitrite ($ONOO^-$), was quantified in the tissues from the RV and LV. The formation of $ONOO^-$ is based on the reaction between ROS and NO. The molecule itself does not have any free radical properties, but it can dissociate rapidly into highly reactive decomposition products.

Comparable to the results obtained for radical staining, no group difference could be detected for the LV concentration of $ONOO^-$. Likewise, the RV had a higher concentration of $ONOO^-$ compared with the left even in the control group. L-NAME substitution led to a further significant increase in peroxynitrite in the RV that could be reduced by tempol to the level of the controls. Captopril, by contrast, led to an additional increase in the $ONOO^-$ concentration in the RV myocardium in the LC group (Fig. 4).

The concentration of malondialdehyde (MDA) in the blood plasma was determined as a general indicator of oxidative stress. The 4-week application of L-NAME led to a 24.2% ± 4.9% (C *vs.* L, $p < 0.05$) increase in plasma MDA levels.

To identify a potential mechanism that explains the different formation in ROS in both ventricles, the expression pattern of antioxidative enzymes was analyzed. In their role as oxidoreductases, SODs catalyze the conversion of superoxide into hydrogen peroxide ($H_2O_2$) and oxygen and thus perform important antioxidant functions. The expression patterns of the three isoforms SOD1, 2, and 3 were each determined separately for the RV and LV of the C and L groups. Only the expression of SOD2 was specifically increased in the LV of L-NAME-substituted animals by 51% ± 3%. In contrast, this isoform was downregulated in the RV by 30% ± 4%. No significant changes could be detected in

TABLE 1. HEART RATE AND RIGHT VENTRICULAR CONTRACTILITY ASSESSMENT *IN VIVO* UNDER ANESTHESIA

| | *Heart rate (bpm)* | *RVSP (mm Hg)* | *RVEDP (mm Hg)* | *RV dp/dt max (mm Hg/s)* | *RV dp/dt min (mm Hg/s)* |
|---|---|---|---|---|---|
| Control (C) | 422 ± 27 | 37.0 ± 5.4 | 2.6 ± 1.6 | 2292 ± 355 | − 2105 ± 395 |
| L-NAME (L) | 391 ± 25 | 30.7 ± 4.6[a] | 0.9 ± 2.2 | 1608 ± 98[a] | − 1363 ± 136[a] |
| L-NAME + captopril (LC) | 397 ± 28 | 35.9 ± 1.0 | 1.8 ± 0.2 | 1925 ± 109[a,b] | − 1486 ± 82[a,b] |
| L-NAME + tempol (LT) | 425 ± 24 | 30.5 ± 1.9[a] | 1.4 ± 1.1 | 1929 ± 47[a,b] | − 1737 ± 90[a,b] |

Changes in RV contractility after 4 weeks. Rats were given pure drinking water (C) $n = 10$, L-NAME (L) $n = 9$, L-NAME plus captopril (LC) $n = 5$ or L-NAME plus tempol (LT) $n = 6$. Data are means ± SD.
[a] $p < 0.05$ *versus* control.
[b] $p < 0.05$ *versus* L-NAME.
bpm, beats per minute; RV, right ventricle; RVEDP, right ventricular end-diastolic pressure; RVSP, right ventricular systolic pressure.

the expression of SOD1 and SOD3 (Fig. 5A). The selective upregulation of SOD2 in the LV of animals fed L-NAME was then confirmed in Western blots (Fig. 5B, C).

An increase in the expression of the transcription factors PGC-1α and nuclear respiratory factor-2 (Nrf-2), which are involved in the regulation of SOD2, was only seen in the LV of the L group. Other downstream targets of Nrf-2 such as glutamate-cysteine ligase, catalytic subunit (Gclc), and thioredoxin reductase 1 (TXNRD1) were also selectively induced in the LV in animals fed L-NAME (Fig. 6A–D).

The catalase, which is also an oxidoreductase that converts any $H_2O_2$ that accumulates to oxygen and water, was upregulated only in the LV similar to SOD2. L-NAME had no effect on the expression of the glutathione peroxidase (Gpx) in either the RV or the LV (Fig. 6E, F).

That there is no change in the expression of the mitochondrial uncouplers UCP2 and UCP3 as well as the hydroxyacyl-CoA dehydrogenase, alpha subunit (HADHA) of the trifunctional protein (MTP) and the transcription factor Nrf-1 indicates that applying L-NAME has no effect on the mitochondrial biogenesis in either the RV or the LV (Supplementary Fig. S3A–D).

Of the two subunits of NADPH oxidase, p22phox and NOX2, only the expression of NOX2 was increased in the LV of rats fed L-NAME (Fig. 6G, H).

### *Effect of L-NAME on cell shortening and SOD2 expression in isolated cardiomyocytes*

To investigate the effect of L-NAME on the contractile behavior and SOD2 expression at a cellular level, cardiomyocytes

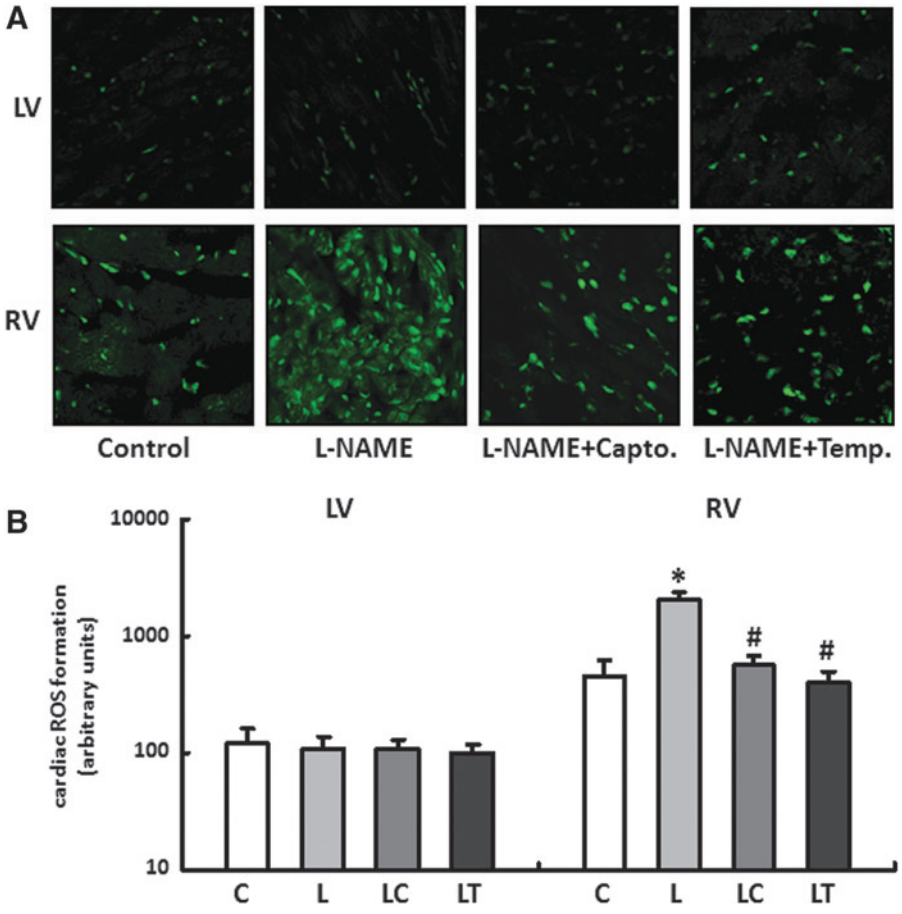


**FIG. 2. (A, B) Generation of superoxide in right and left ventricles.** Dihydroethidium (DHE) staining was performed to measure the formation of reactive oxygen species in heart tissue from RV and LV of all treatment groups (control [C], L-NAME [L], L-NAME plus captopril [LC] and L-NAME plus tempol [LT]). Slides were imaged by confocal microscopy using an excitation wavelength of 488 nm and an emission wavelength of 540 nm. Data are means ± SD of $n = 5$ hearts. $^{*}p < 0.05$ *versus* control, $^{\#}p < 0.05$ *versus* L-NAME.

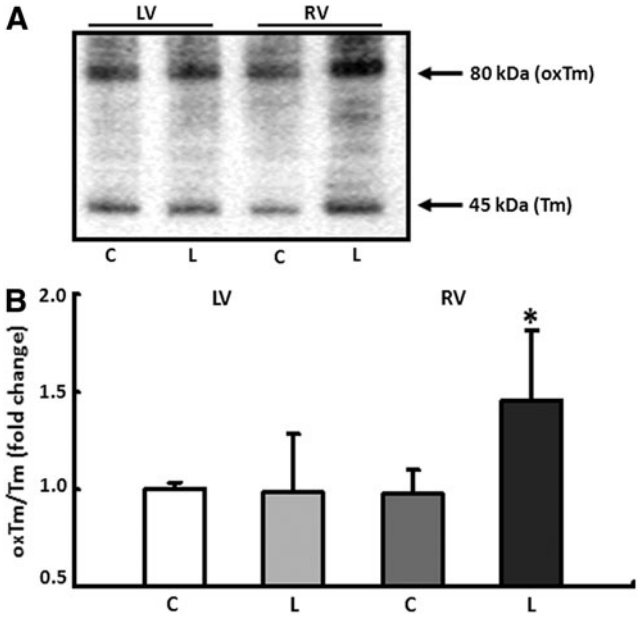


**FIG. 3. Conformational changes of tropomyosin (Tm) induced by oxidative stress. (A)** Quantification of disulphide cross-bridge formation in tropomyosin (Tm) under non-reducing conditions. Oxidative modification of Tm (oxTm) leads to dimerization of the protein and was detected as a high-molecular-weight peptide of ~80 kDa. **(B)** Protein expression was analyzed in the RV and LV of control (C) and L-NAME fed animals (L). Results are given as ratio of oxTm to Tm. Data are means ± SD of $n = 4$ hearts. *$p < 0.05$ *versus* control.

were isolated separately from the RV and LV of untreated rats and incubated for 24 h with L-NAME. Compared with untreated control cells, L-NAME led to a significant reduction in the relative cell shortening only in the RV myocytes. The expression of SOD2 corresponded to the *in vivo* results previously described (Fig. 7A–C). Accordingly, L-NAME led to an increase in mitochondrial ROS formation only in RV myocytes as detected by mitochondria-targeted superoxide fluorescent indicator MitoSOX Red (Supplementary Fig. S4).

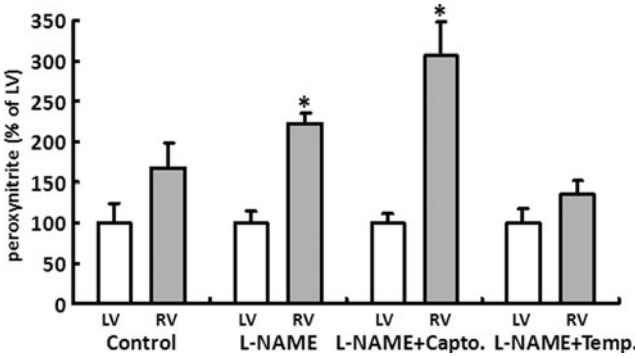


**FIG. 4. L-NAME induced changes in the formation of peroxynitrite ($ONOO^-$).** $ONOO^-$ was measured in heart tissue from RV (*gray bars*) and LV (*white bars*) of all treatment groups (control [C], L-NAME [L], L-NAME plus captopril [LC], and L-NAME plus tempol [LT]). Average LV concentration of $ONOO^-$ was 0.65 ± 0.21 ng/mg protein. Values of RV are displayed as percent of LV. Data are means ± SD of $n = 4$ hearts. *$p < 0.05$ *versus* LV.

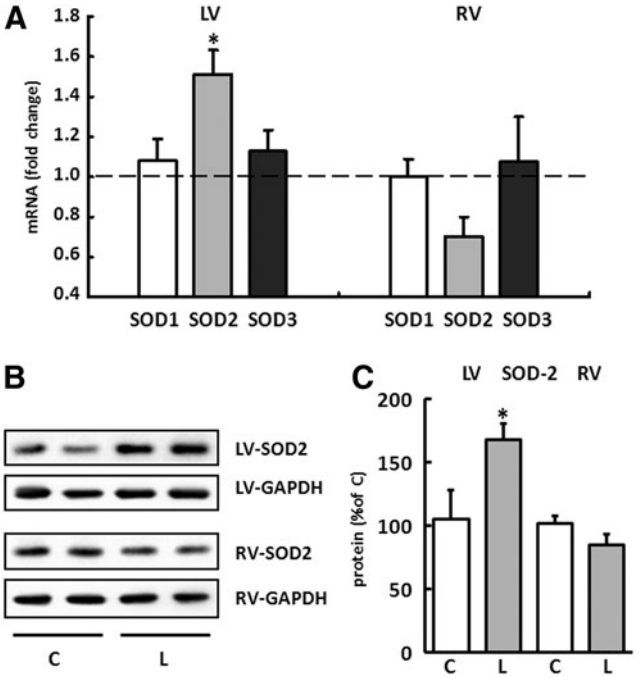


**FIG. 5. Expression pattern of superoxide dismutases (SOD) in right and left ventricles. (A)** The expression for SOD1, SOD2, and SOD3 was analyzed separately for the RV and LV of drinking-water controls and L-NAME-fed animals. Results are displayed as fold change for each isoform normalized to the control group (*dashed line*). The expression of hypoxanthine-guanine phosphoribosyltransferase (HPRT) was used for normalization. Data are means ± SEM of $n = 8$ hearts. **(B)** Representative immunoblots indicating SOD2 immunoreactivity in the RV and LV from control (C) and L-NAME (L)-treated animals. SOD2 values were normalized to GAPDH levels. **(C)** Densitometric analysis of immunoblot bands. SOD2 was significantly increased in the LV from L-NAME fed animals (*gray bar*) compared with control animals (*white bar*). Data are means ± SD of $n = 5$ hearts. *$p < 0.05$ *versus* control.

The cell shortening seen in the LV cardiomyocytes was significantly reduced if the myocytes incubated with L-NAME were also incubated with the translation inhibitor cycloheximide, the transcription inhibitor actinomycin D, or the Sirt1 inhibitor Ex-527 (Fig. 7D). Under these conditions, the induction of the SOD2 expression failed to materialize (Fig. 7A, B). The MAP kinase inhibitor PD98059 did not have any effect on the cell contraction.

### *Effect of L-NAME on the cardiac remodeling of the extracellular matrix*

Finally, the development and induction of cardiac fibrosis was analyzed in response to the different level of ROS in the RV and LV.

The causal involvement of the cytokine transforming growth factor beta1 (TGF-beta1) in the progression of chronic cardiac insufficiency has already been well documented. It also plays a critical role in the development and maintenance of cardiac fibrosis.

The expression patterns for TGF-beta1 and the extracellular matrix proteins collagen I and collagen III were analyzed separately for the RV and LV using real-time reverse transcription polymerase chain reaction (RT-PCR). In the LV, only the

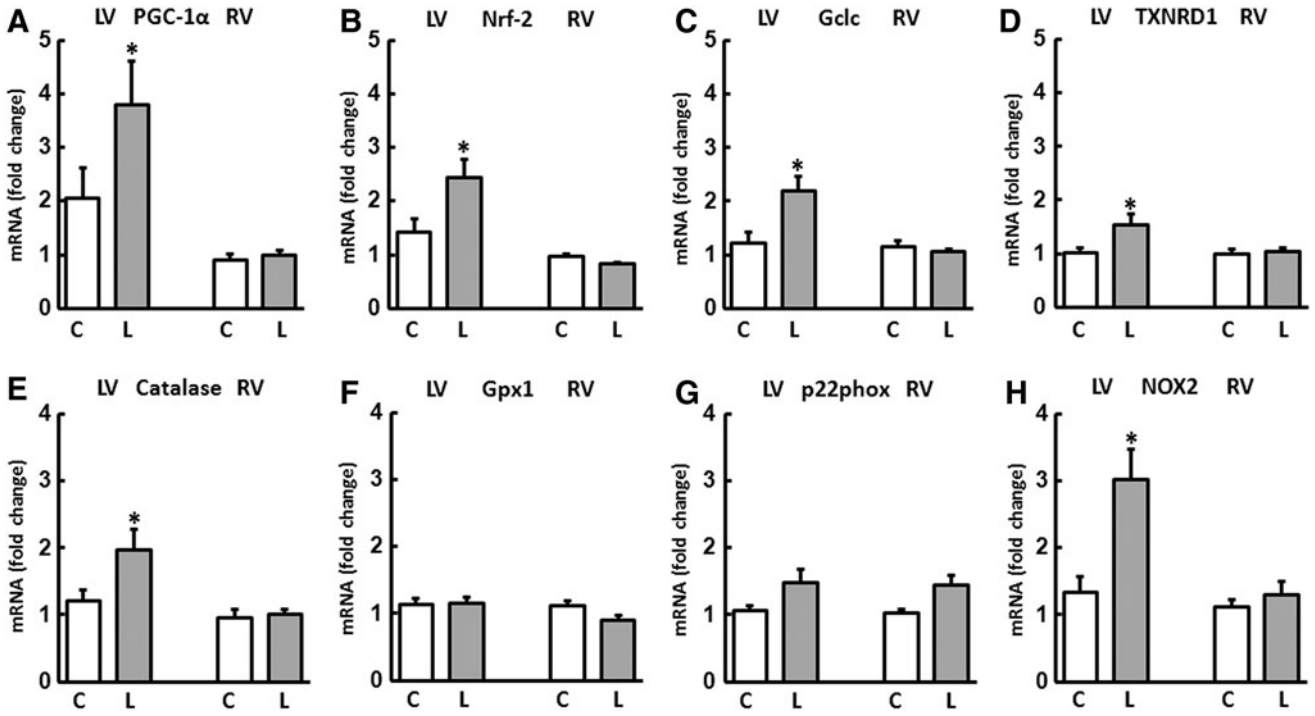


**FIG. 6. Regulation of genes involved in redox homeostasis and antioxidative defense.** The expression of mRNA was analyzed in the RV and LV of control (C) and L-NAME (L)-fed animals. The transcription factors **(A)** PGC-1α and **(B)** nuclear respiratory factor-2 (Nrf-2) as well as their downstream targets **(C)** glutamate cysteine ligase (Gclc) and **(D)** thioredoxin reductase 1 (TXNRD1) were selectively induced in the LV of L-NAME fed animals. L-NAME also induced the expression of **(E)** catalase in the LV but had no effect on the expression of **(F)** glutathione peroxidase 1 (Gpx1). Expression of **(G)** p22phox was not influenced but that of **(H)** NOX2 was induced by L-NAME in the LV. Data are means ± SD of $n = 8$ hearts. $^*p < 0.05$ *versus* control.

expression of TGF-beta1 was reduced in L-NAME fed animals by 19% ± 3% compared with their drinking-water controls. In the LC and LT groups, no change could be detected in the expression of any of the genes investigated. In contrast to the normal finding in the LV, TGF-beta1 was upregulated in the RV in the L group by 102% ± 6%. The expression of collagen I was increased by 156% ± 16%, and that of collagen III was increased by 280% ± 26%. Both the increase in the TGF-beta1 and the induction of the two collagen isoforms could be significantly reduced by captopril and tempol (Fig. 8A–C).

The massive upregulation of the collagen in the RV of L-NAME-fed animals could subsequently be confirmed using Sirius Red staining in histological sections. Qualitatively, the areas close to the interventricular septum were particularly affected by an increased incorporation of extracellular matrix proteins. Localization of the fibrosis along the RV circumference was limited primarily to endocardial and epicardial compartments (Fig. 8D, E).

However, when the antihypertensive hydralazine was combined with L-NAME after 2 weeks of L-NAME treatment, the blood pressure fell from 160 ± 6 mm Hg (after 2 weeks of L-NAME) to 126 ± 5 mm Hg. However, due to the inability of hydralazine to prevent L-NAME-induced $O_2^{-\bullet}$ production, the hearts from this group also displayed a significant upregulation of TGF-beta1 only in the RV (Supplementary Fig. S5).

### *The structural remodeling of the RV and LV in eNOS$^{-/-}$ mice*

To validate results obtained from L-NAME experiments, eNOS$^{-/-}$ mice were used as another model for a chronic deficiency in NO. Comparable to the mRNA expression pattern in the RV and LV of L-NAME fed animals, SOD2 was upregulated only in the LV of eNOS$^{-/-}$ mice, whereas the expression of TGF-beta1 and collagen I did not change in the LV but was significantly increased in the RV (Supplementary Fig. S6).

## Discussion

The state of chronically reduced bioavailability of NO is a risk factor for the entire cardiovascular system, which can be attributed to the increased hemodynamic, oxidative, and fibrotic stress. In this study, the conditions were created for a corresponding scenario in 3-month-old female Wistar rats by feeding them the nonspecific NOS inhibitor L-NAME. Once the 4-week treatment period was complete, the cardiac remodeling was characterized separately for the RV and LV while considering the structural and functional adaptive responses.

Unlike the LV, the RV did not display the necessary adaptive mechanisms to cope with increased oxidative stress, the main and new finding of this study. The radical load induced by L-NAME in the RV myocardium led to the formation of a dilated cardiomyopathy with pronounced contractile dysfunction and cardiac fibrosis. The endogenous antioxidant potential prevented a corresponding structural and functional remodeling in the LV. Using adjuvant therapy with the SOD-mimetic tempol or captopril, which also has an antioxidative effect, the vicious cycle of free radical generation, fibrosis, and contractile dysfunction could be disrupted in the RV. Using the model of isolated cardiomyocytes, it

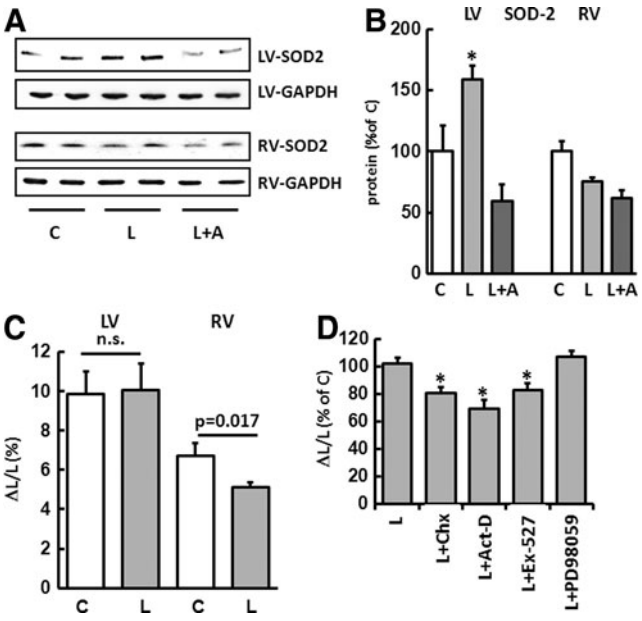


**FIG. 7. Effects of L-NAME on SOD2 expression and cell shortening at a cellular level. (A)** Representative immunoblots indicating SOD2 immunoreactivity in isolated cardiomyocytes from untreated control cells (C), cells incubated for 24 h with L-NAME (L) and L-NAME plus actinomycin D (L + A). SOD2 values were normalized to GAPDH levels. **(B)** Densitometric analysis of immunoblot bands. SOD2 was upregulated only in myocytes isolated from the LV. Data are means ± SD of $n = 4$ hearts. **(C)** Effect of L-NAME on cell shortening. Cardiomyocytes were isolated separately from the RV and LV of untreated rats and incubated with L-NAME for 24 h. L-NAME led to a significant reduction in relative cell shortening only in RV myocytes. Data are means ± SD of $n = 4$ hearts. **(D)** Cell shortening of LV cardiomyocytes was significantly reduced if myocytes were co-incubated with L-NAME (L) and the translation inhibitor cycloheximide (L + Chx), the transcription inhibitor actinomycin D (L + Act-D), or the Sirt1 inhibitor Ex-527 (L + Ex-527). PD98059 (L + PD98059) did not have any effect on cell contraction. Data are means ± SD of $n = 4$ hearts. $^*p < 0.05$ *versus* control.

could also be shown that the specific endogenous properties of RV myocytes were critically involved in the diagnosed RV dysfunction.

In general, the RV is characterized by a high degree of plasticity. If it detects systemic perfusion due to a patent arterial duct while still in the uterus, this function is transferred from birth onward to the left half of the heart (26). The myocardium of the RV adjusts postpartum to its new function and is characterized from this point on by a high degree of elasticity due to the low wall thickness. The structure and geometry are designed for volume work and can adjust more easily to an increased preload than to an increase in the afterload (26).

The contribution of the RV to maintaining appropriate blood circulation was underestimated for many years, and research into its specific physiology was neglected. However, its importance for the entire cardiovascular system can be explained solely by the fact that physical performance correlates more strongly with RV function than with LV function (4).

Gulati *et al.* diagnosed an RV dysfunction in 30% of patients with nonischemic dilated cardiomyopathy and identified this as an independent risk factor that was associated with a fourfold higher total mortality (24). Comparable results were obtained by Mehta *et al.* for the involvement of the RV in LV myocardial infarction, and they describe an increased rate of postischemic complications and fatalities (35). For pulmonary hypertension, the right heart function was even identified as a critical predictor for premature mortality, although the RV has the potential to adjust in the long term to a pathologically increased afterload by means of compensatory hypertrophy (25).

The chronic application of L-NAME in drinking water is an established model for arterial hypertension. The increased vascular resistance and the vascular remodeling are induced by a lowering of the NO level and activation of the systemic and local renin–angiotensin systems as well as greater oxidative stress (23). The therapeutic use of the ACE-inhibitor captopril led to a significant fall in the systolic blood pressure, while the antioxidant tempol was only able to prevent a further increase in the last 2 weeks.

The involvement of ROS in cardiovascular effects induced by L-NAME has already been demonstrated by Kumar *et al.*, who were even able to significantly lower the blood pressure using oral application of syringic acid, a naturally occurring antioxidant (30). A reduction of oxidative stress through selective inhibition of xanthine oxidase by allopurinol had no effect on hypertension but significantly improved the L-NAME-induced cardiac remodeling (28). The significantly elevated plasma MDA levels, which can be attributed to an increase in the lipid peroxidation, suggest that chronic application of L-NAME also led to an increase in radical stress in the model used here.

However, histological and molecular results indicate that the cause of the RV dysfunction is a massive increase in oxidative stress. NADPH oxidase, xanthine oxidase, and the renin–angiotensin system were identified as potential sources of excessive radical production under chronic L-NAME application (46). ROS, generated by NADPH oxidases, also induce the formation of ROS in mitochondria, which, in turn, stimulate radical production in the cytosol, thus inducing a self-sustaining vicious cycle (17, 38, 40). A targeted pharmacological intervention using substances with an antioxidant potential specific for mitochondrial ROS disrupts this feed-forward cycle efficiently (44).

This therapeutic approach corresponds to the endogenous upregulation of SOD2 in the LV of animals treated with L-NAME. The type 2 isoform of SOD, which is also known as manganese superoxide dismutase (Mn-SOD), catalyzes the formation of $H_2O_2$ from superoxide anions, specifically in the mitochondria.

As a direct consequence of the RV radical load, the induction of the cytokine TGF-beta is a key mechanism that is responsible for the development of fibrosis and RV failure (12, 27, 31).

In addition to RV fibrosis, which primarily affects ventricular stiffness and thus diastolic filling, a higher degree of oxidized Tm (oxTm) could be identified in RV of animals fed L-NAME. The formation of DCB induced by oxidative stress leads to a conformational change of Tm protein, which directly affects contractile function. However, the observed modification of Tm in RV of L-NAME-fed animals is likely to be responsible for the deterioration in RV systolic pressure as well as for the reduction in dp/dt max and dp/dt min (14, 15).

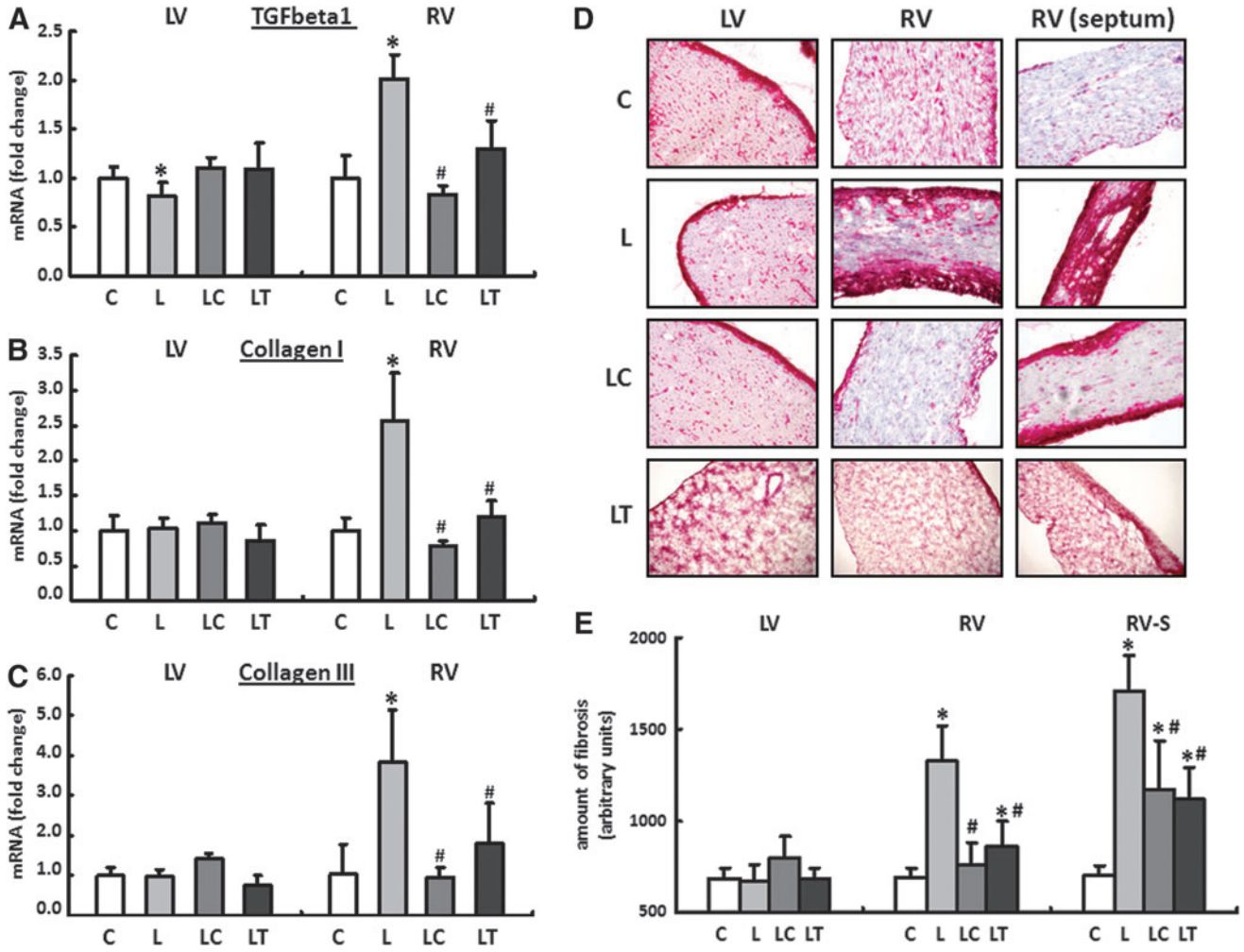


**FIG. 8. Cardiac remodeling of the extracellular matrix.** The mRNA expression for **(A)** transforming growth factor beta1 (TGF-beta1), **(B)** collagen I, and **(C)** collagen III was analyzed in all four treatment groups separately for the RV and LV using real-time reverse transcription polymerase chain reaction (RT-PCR). Rats were given pure drinking water (C), L-NAME (L), L-NAME plus captopril (LC), and L-NAME plus tempol (LT). The expression of HPRT was used for normalization. Data are means ± SEM of $n = 8$ hearts. **(D, E)** The massive upregulation of collagen I and III in the RV of L-NAME-fed animals (L) could be confirmed subsequently in histological sections with the help of Sirius Red staining. RV fibrosis could be significantly reduced by captopril (LC group) or tempol (LT group). RV (septum): RV close to the septum interventricularis. Data are means ± SD of $n = 5$ hearts. $^{*}p < 0.05$ *versus* control, $^{\#}p < 0.05$ *versus* L-NAME.

The missing upregulation of SODs in the RV together with the accumulation of $O_2^{-\bullet}$ have also led to a selective increase in peroxynitrite in the RV of animals fed L-NAME.

The intrinsically higher RV $ONOO^-$ concentration compared with the LV conforms to the results obtained with the DHE-based radical staining. The induction of the LV TXNRD1 expression described is critically involved in the detoxification of $ONOO^-$ by making peroxiredoxin available.

The significant reduction in free radicals achieved by tempol, therefore, also led to a normalization of the $ONOO^-$ concentration in the RV in the LT group. Because both ROS and NO are required for the formation of $ONOO^-$, the increase in peroxynitrite in the RV of the LC group could possibly be explained by the stimulatory effect of captopril on NO production. The inhibitory effect on the RAS, direct antioxidative effects, and the increased formation of NO are some of the protective properties of captopril that can generally contribute to a reduction in oxidative stress (9, 22). To what extent the increased formation of $ONOO^-$ in the RV of the LC group influences structural or functional remodeling cannot be determined based on the current data. Furthermore, the significance of $ONOO^-$ as an exclusively harmful compound is in doubt, and its involvement in the maintenance of the redox homeostasis and stress adaptation is the subject of ongoing discussion (3, 19, 20).

The inability of the RV to appropriately adjust its antioxidant capacity under pathophysiological conditions caused by L-NAME or an eNOS knockout led to an increase in the formation of free radicals (DHE staining, MitoSox Red), an increased percentage of oxTm, and a rise in the formation of peroxynitrite. The causes of the resultant cardiac dysfunction are based on a structurally remodeled ventricle with a significantly increased quantity of collagen and the impaired function of the RV cardiomyocytes themselves. The restrictive components of the cardiac symptoms led to an increase in the liver transaminases GOT/GPT *via* blood accumulation in the liver.

The LV was able to critically elevate its antioxidant potential by inducing PGC-1α and its downstream target Nrf-2 (10). Nrf-2 dependent genes, which include the cytoprotective proteins Gclc and TXNRD1 along with SOD2, prevented both the structural remodeling and the impaired function of the LV myocardium (11, 18). The transcription of PGC-1α is, in turn, regulated by Sirt1, the inhibition of which by Ex-527 led to a reduction in the cell shortening of LV isolated myocytes as did the inhibition of transcription by actinomycin D (Act-D) and the inhibition of translation by Chx. The previously described upregulation of SOD2 was prevented by a blockade of this signaling pathway.

Both therapeutic interventions, captopril and tempol, had an equally positive effect on the cardiac remodeling of the RV independent of their antihypertensive efficiency. Moreover, hydralazine with strong antihypertensive but no antioxidative properties was unable to prevent the induction of the RV remodeling (6). These results support the conjecture that neither the blood pressure nor an elevated afterload but rather ROS is the cause of the RV symptoms. This situation is supported by the results of the cell culture experiments that confirmed the impaired adaptation mechanisms (reduced SOD2 expression) and the resulting impaired function of the RV myocardium independent of systemic influences and blood pressure.

To what extent the application of L-NAME affected the pulmonary arterial pressure was not determined in this study. Sekiguchi *et al.* compared the peripheral and pulmonary arterial blood pressure in spontaneously hypertensive rats and rats fed L-NAME (2 weeks, 50 mg/100 ml). Systemic hypertension was recorded in both models. An increase in the pulmonary arterial pressure could, however, only be diagnosed in the spontaneously hypertensive rats (SHR), while the chronic application of L-NAME did not have any effect on the pressure ratios in the pulmonary circulation system (43). These results correspond to the expression pattern described in this study for the natriuretic peptide ANP. The increased afterload in the LV, associated with a moderate hypertrophy, led to a significant increase in the LV ANP expression. The lack of induction of ANP expression in the RV myocardium indicates that the pressure conditions in the pulmonary circulation are unchanged.

In light of this, the results of this study can be translated to cardiac diseases that are associated with elevated oxidative stress and, subsequently, can induce the development of RV failure (10). Without itself being the starting point of the symptoms, for the RV there is an elevated risk of being secondarily damaged due to increased accumulation of ROS during LV failure or LV infarction.

In summary, the results of this study show for the first time that oxidative stress is a vastly greater risk factor for the RV than for the LV. Molecular and cellular results indicate that critical signaling pathways and key enzymes in the RV and LV are activated and regulated in different ways, which may lead to the development of targeted therapy against RV failure. Indeed, our results suggest that the prognosis for RV failure can be greatly improved by using ACE inhibitors with high antioxidant capacity.

## Materials and Methods

The investigation conforms the Guide for the Care and Use of Laboratory Animals published by the US National Institute of Health (NIH Publication No. 85-23, revised 1996). The study was approved by the local authorities for animal experiments (V54-19c 2015 (I) GI 20/1 Nr. 58-2005).

### *Experimental model*

Eighty-two 3-month-old female wistar rats were divided into four groups and kept in individual cages. Animals had free access to food and water *ad libitum*. Animals were assigned to receive L-NAME (7.5 mg/day in drinking-water), L-NAME plus captopril (5.0 mg/day in drinking-water) (2), L-NAME plus tempol (1.0 m*M* in drinking-water) (5), L-NAME plus hydralazine (5.0 mg/day in drinking-water) (42), or drinking-water only (age-matched control) for 28 days (Supplementary Fig. S1A). As an alternative model for a chronic deficiency in NO, 6-month-old female $eNOS^{-/-}$ mice and their wild-type littermates were used.

The health status of the experimental animals was determined weekly using a ''distress score'' (33). Over the entire experimental period, no animals died or had to be excluded from the study based on the exclusion criteria.

### *Determination of the blood pressure and heart rate*

Peak systolic blood pressure and heart rate were measured weekly using the non-invasive tail-cuff method (TSE-Systems, 209000Series). Before the start of the study, the animals were adjusted to the experimental procedure over 1 week. The mean of 10 consecutive blood pressure readings was obtained for each animal at weekly intervals.

### *RNA isolation and real-time RT-PCR*

Total RNA was isolated from RV and LV using peqGold TriFast (peqlab; Biotechnologie GmbH) according to the manufacturer's protocol. To remove genomic DNA contamination, isolated RNA samples were treated with 1 U DNase/μg RNA (Invitrogen) for 15 min at 37°C. One μg of total RNA was used in a 10 μl reaction to synthesize cDNA using Superscript RNaseH Reverse Transcriptase (200 U/μg RNA; Invitrogen) and oligo dTs as primers. RT reactions were performed for 50 min at 37°C. Real-time quantitative PCR was performed using the MyiQ® detection system (Bio-Rad) in combination with the iTaq Universal SYBR Green Real-Time PCR Supermix (Bio-Rad). Quantification was performed as described earlier (32). Primer sequences are listed in Supplementary Table S4.

### *Picrosirius red staining*

Samples were embedded with Tissue-Tek® (Sakura) and sectioned in 10 μm slices. Histological sections were fixed in Bouin solution and subsequently stained in 0.1% (wt/vol) Sirius Red solution (Sigma-Aldrich Chemie). Sections were washed by 0.01 N HCl, Aqua dest. and counterstained for nuclei by Mayers hemalaun solution, washed with Aqua dest. for 5 min, and dehydrated with ethanol. Total collagen content was quantified by digital image analysis using Leica Confocal Software Lite Version (LCS Lite). The mean of $n = 5$ preparations was used to quantify the extent of interstitial fibrosis.

### *Measurement of superoxide*

To perform DHE staining, cryosections of RV and LV were incubated with DHE (dissolved in 1 X PBS) for 10 min

at 37°C in a light-protected humidity chamber, then fixed with Dako Fluorescent Mounting Medium (Dako, North America, Inc.). Slides were then imaged by confocal microscopy (LSM 510 META; Carl Zeiss) using an excitation wavelength of 488 nm; emission was recorded at 540 nm (37).

Analysis was performed by digital image analysis using Leica Confocal Software Lite Version (LCS Lite). The mean fluorescence intensity of $n = 5$ ventricles was used to quantify the extent of superoxide.

### *Mitochondrial ROS analysis*

Formation of ROS in mitochondria was detected with MitoSOX Red, a mitochondrial superoxide fluorescence indicator. Briefly, isolated cardiomyocytes were incubated with 1 $\mu M$ MitoSOX Red at 37°C for 30 min and then washed twice for 10 min in CCT medium. The loaded cells were excited at 510 nm, and the emitted light was collected at 580 nm (1).

### *Detection of MDA using a TBARS Assay Kit*

The formation of MDA was used as a well-established indicator of oxidative stress in plasma samples. Shortly, blood samples from treated and untreated rats were centrifuged (1500 *g*) at 4°C for 15 min to obtain plasma. One hundred microliters sample was incubated with TBA under acid conditions for 60 min at 95°C. Sample vials were then placed on ice for 10 min and centrifuged for 10 min at 1600 *g*. One hundred fifty microliters reaction mixture was measured fluorometrically in duplicate at an excitation wavelength of 530 nm and an emission wavelength of 550 nm. The tests were carried out using TBARS Assay Kit purchased from Cayman Chemical Company.

### *Measurement of peroxynitrite*

To estimate peroxynitrite formation in the RV and LV, we measured peroxynitrite marker nitrotyrosine by ELISA (components from Cayman Chemical) in ventricular homogenates as previously described (8, 16). Briefly, RV and LV tissue samples were pulverized in liquid nitrogen, sonicated in 4× homogenization buffer, and centrifuged. Supernatants were then incubated overnight with anti-nitrotyrosine rabbit IgG and nitrotyrosine acetylcholinesterase tracer in precoated (mouse anti-rabbit IgG) microplates followed by development with Ellman's reagent. Protein concentration of the samples was measured by the bicinchoninic acid assay.

### *Western blot*

Total protein was extracted from RV and LV using Cell Lysis Buffer (10×) (Cell Signaling) according to the manufacturer's protocol. Briefly, the homogenate was centrifuged at 14,000 g at 4°C for 10 min and the supernatant was treated with Laemmli buffer. Protein samples were loaded on NuPAGE Bis-Tris Precast gels (10%; Life Technology) and, subsequently, transferred onto nitrocellulose membranes. Blots were incubated with one of the following antibodies: anti-Tm purchased from Sigma-Aldrich (product T9283) or anti SOD2 purchased from Merck Millipore (product 06-984). Secondary antibodies [horseradish peroxidase (HRP)-conjugated] directed against rabbit IgG or mouse IgG were purchased from Sigma-Aldrich, respectively Affinity Biologicals.

### *Hemodynamic measurements*

Heart function was measured in closed-chest spontaneously breathing rats anesthetized with thiopental sodium (Trapanal® 60 mg/kg i.p.) using ultraminiature catheter pressure transducers (3 F; Millar Instruments, Inc.). Briefly, the rats were placed in supine position on a heating pad and the RV catheter (model SPR-291) was inserted into the right jugular vein and advanced into the RV *via* the right atrium. Heart rate, RV systolic pressure, and the rate in rise and fall of ventricular pressure (RV dp/dt) were recorded continuously on a PC at a sampling rate of 1 kHz using PowerLab 16/30 with Quad Bridge Amp and LabChart 7 software (all ADInstruments) for 10–15 min.

### *Langendorff perfusion*

To analyze LV function, conditioned rats were anaesthetized by isoflurane and killed by cervical dislocation. Thereafter, hearts were rapidly excised and the aorta was cannulated for retrograde perfusion with a 16-gauge needle connected to a Langendorff perfusion system. A polyvinyl chloride balloon was inserted into the LV through the mitral valve and held in place by a suture tied around the left atrium. The other end of the tubing was connected to a pressure transducer for continuous measurement of LV pressure, dp/dt max, and dp/dt min (41).

### *Measurements of transaminases (GOT/GPT) in blood plasma*

To quantify GOT/GPT levels in plasma samples, the rat aspartate aminotransferase ELISA Kit from Bioassay Technology Laboratory was used. The test procedure was performed according to the manufacturer's instructions. Briefly, blood samples from treated and untreated rats were centrifuged (1500 *g*) for 15 min to obtain plasma. Forty microliters of plasma were then incubated in duplicate with 10 $\mu$l biotin-labeled anti GOT/GPT antibodies and streptavidin-HRP. The liquid turned blue after adding chromogen solution and yellow with the effect of acid. The color intensity correlates positively with the concentration of GOT/GPT.

### *Isolation and cultivation of cardiomyocytes from the RV and LV*

Heart muscle cells from the RV and LV were isolated from 3-month-old male wistar rats. Briefly, hearts were excised, transferred rapidly to ice-cold saline, and mounted on the cannula of a Langendorff perfusion system. Heart perfusion and subsequent steps were performed at 37°C. First, hearts were perfused in a non-circulating manner for 5 min at 10 ml/min. Thereafter, perfusion was continued with recirculation using 50 ml perfusate supplemented with 0.06% (w/v) crude collagenase and 25 $\mu M$ $CaCl_2$ at 5 ml/min for 25 min. Then, the RV was dissected from the LV and septum and processed separately in the next few steps (47).

Isolated cardiomyocytes were then incubated with L-NAME (1.0 m$M$; Sigma-Aldrich, product N5751) alone and in the presence of cyclohexemide (35.0 $\mu M$; Sigma-Aldrich, product C-7698), actinomycin D (5.0 $\mu M$; Sigma-Aldrich, product A5142), Ex-527 (10.0 $\mu M$; Sigma-Aldrich, product E7034), or PD98059 (10.0 $\mu M$; Merck Millipore, product 513000) for 24 h.

### *Determination of cell contraction*

Cell shortening was measured as described earlier in greater detail (47). Briefly, isolated cardiomyocytes were allowed to contract at room temperature and analyzed using a cell-edge detection system. Cells were stimulated *via* two AgCl electrodes with biphasic electrical stimuli composed of two equal but opposite rectangular 50-V stimuli of 0.5 ms duration. Each cell was stimulated for 1 min at a frequency of 2.0 Hz. Every 15 s contractions were recorded. The mean of these four measurements was used to define the cell shortening of a given cell. Cell lengths were measured *via* a line camera (data recording at 500 Hz). Data are expressed as cell shortening normalized to diastolic cell length (dL/L [%]).

### *Statistics*

Data are expressed as indicated in the legends. ANOVA and the Student–Newman–Keuls test for *post hoc* analysis were used to analyze experiments in which more than one group was compared. In cases in which two groups were compared, Student's *t*-test or Mann–Whitney test was employed, depending on a normal distribution of samples (Levene test). $p < 0.05$ was regarded as significant.

## Acknowledgments

The study was supported by the Deutsche Forschungsgemeinschaft (DFG) and received funding through the Excellence Cluster Cardio-Pulmonary System (ECCPS, Giessen). C.C. holds a János Bolyai fellowship; P.F. is a Szentágothai Fellow of the National Program of Excellence (Grant TAMOP 4.2.4.A/2-11-1-2012-0001).

## Author Disclosure Statement

No competing financial interests exist.

## References

1. Abdallah Y, Kasseckert SA, Iraqi W, Said M, Shahzad T, Erdogan A, Neuhof C, Gündüz D, Schlüter KD, Tillmanns H, Piper HM, Reusch HP, and Ladilov Y. Interplay between $Ca^{2+}$ cycling and mitochondrial permeability transition pores promotes reperfusion-induced injury of cardiac myocytes. J Cell Mol Med 15: 2478–2485, 2011.
2. Amazonas R, de Almeida Sanita R, Kawachi H, and Lopes de Faria J. Prevention of hypertension with or without renin-angiotensin system inhibition precludes nephrin loss in the early stage of experimental diabetes mellitus. Nephron Physiol 107: 57–64, 2007.
3. Andreadou I, Iliodromitis EK, Rassaf T, Schulz R, Papapetropoulos A, and Ferdinandy P. The role of gasotransmitters NO, $H_2S$, CO in myocardial ischemia/reperfusion injury and cardioprotection by preconditioning, postconditioning, and remote conditioning. Br J Pharmacol 2014 doi: 10.1111/bph.12811.
4. Baker BJ, Wilen MM, Boyd CM, Dinh H, and Franciosa JA. Relation of right ventricular ejection fraction to exercise capacity in chronic left ventricular failure. Am J Cardiol 54: 596–599, 1984.
5. Banday AA, Marwaha A, Tallam LS, and Lokhandwala MF. Tempol reduces oxidative stress, improves insulin sensitivity, decreases renal dopamine D1 receptor hyperphosphorylation, and restores D1 receptor-G-protein coupling and function in obese Zucker rats. Diabetes 54: 2219–2226, 2005.
6. Bauersachs J, Bouloumié A, Fraccarollo D, Hu K, Busse R, and Ertl G. Hydralazine prevents endothelial dysfunction, but not the increase in superoxide production in nitric oxide-deficient hypertension. Eur J Pharmacol 362: 77–81, 1998.
7. Baylis C. Nitric oxide deficiency in chronic kidney disease. Am J Physiol Renal Physiol 294: 1–9, 2008.
8. Bencsik P, Kupai K, Giricz Z, Görbe A, Pipis J, Murlasits Z, Kocsis GF, Varga-Orvos Z, Puskás LG, Csonka C, Csont T, and Ferdinandy P. Role of iNOS and peroxynitrite-matrix metalloproteinase-2 signaling in myocardial late preconditioning in rats. Am J Physiol Heart Circ Physiol 299: 512–518, 2010.
9. Benzie IF and Tomlinson B. Antioxidant power of angiotensin-converting enzyme inhibitors *in vitro*. Br J Clin Pharmacol 45: 168–169, 1998.
10. Borchi E, Bargelli V, Stillitano F, Giordano C, Sebastiani M, Nassi PA, d'Amati G, Cerbai E, and Nediani C. Enhanced ROS production by NADPH oxidase is correlated to changes in antioxidant enzyme activity in human heart failure. Biochim Biophys Acta 1802: 331–338, 2010.
11. Buelna-Chontal M, Guevara-Chávez JG, Silva-Palacios A, Medina-Campos ON, Pedraza-Chaverri J, and Zazueta C. Nrf2-regulated antioxidant response is activated by protein kinase C in postconditioned rat hearts. Free Radic Biol Med 74: 145–156, 2014.
12. Bujak M and Frangogiannis NG. The role of TGF-$\beta$ signaling in myocardial infarction and cardiac remodeling. Cardiovasc Res 74: 184–195, 2007.
13. Cannon RO 3rd. Role of nitric oxide in cardiovascular disease: focus on the endothelium. Clin Chem 44: 1809–1819, 1998.
14. Canton M, Skyschally A, Menabò R, Boengler K, Gres P, Schulz R, Haude M, Erbel R, Di Lisa F, and Heusch G. Oxidative modification of tropomyosin and myocardial dysfunction following coronary microembolization. Eur Heart J 27: 875–881, 2006.
15. Canton M, Menazza S, Sheeran FL, Polverino de Laureto P, Di Lisa F, and Pepe S. Oxidation of myofibrillar proteins in human heart failure. J Am Coll Cardiol 57: 300–309, 2011.
16. Csont T, Csonka C, Onody A, Gorbe A, Dux L, Schulz R, Baxter GF, and Ferdinandy P. Nitrate tolerance does not increase production of peroxynitrite in the heart. Am J Physiol Heart Circ Physiol 283: 69–76, 2002.
17. Dikalov S. Cross talk between mitochondria and NADPH oxidases. Free Radic Biol Med 51: 1289–1301, 2011.
18. Do MT, Kim HG, Choi JH, and Jeong HG. Metformin induces microRNA-34a to downregulate the Sirt1/Pgc-1$\alpha$/Nrf2 pathway, leading to increased susceptibility of wild-type p53 cancer cells to oxidative stress and therapeutic agents. Free Radic Biol Med 74: 21–34, 2014.
19. Ferdinandy P. Peroxynitrite: just an oxidative/nitrosative stressor or a physiological regulator as well? Br J Pharmacol 148: 1–3, 2006.
20. Ferdinandy P and Schulz R. Nitric oxide, superoxide, and peroxynitrite in myocardial ischaemia-reperfusion injury and preconditioning. Br J Pharmacol 138: 532–543, 2003.
21. Gaucher C, Boudier A, Dahboul F, Parent M, and Leroy P. S-nitrosation/denitrosation in cardiovascular pathologies: facts and concepts for the rational design of S-nitrosothiols. Curr Pharm Des 19: 458–472, 2013.
22. Gauthier KM, Cepura CJ, and Campbell WB. ACE inhibition enhances bradykinin relaxations through nitric oxide

and B1 receptor activation in bovine coronary arteries. Biol Chem 394: 1205–1212, 2013.
23. Gonzalez W, Fontaine V, Pueyo ME, Laquay N, Messika-Zeitoun D, Philippe M, Arnal JF, Jacob MP, and Michel JB. Molecular plasticity of vascular wall during N(G)-nitro-L-arginine methyl ester-induced hypertension: modulation of proinflammatory signals. Hypertension 36: 103–109, 2000.
24. Gulati A, Ismail TF, Jabbour A, Alpendurada F, Guha K, Ismail NA, Raza S, Khwaja J, Brown TD, Morarji K, Liodakis E, Roughton M, Wage R, Pakrashi TC, Sharma R, Carpenter JP, Cook SA, Cowie MR, Assomull RG, Pennell DJ, and Prasad SK. The prevalence and prognostic significance of right ventricular systolic dysfunction in nonischemic dilated cardiomyopathy. Circulation 128: 1623–1633, 2013.
25. Handoko ML, de Man FS, Allaart CP, Paulus WJ, Westerhof N, and Vonk-Noordegraaf A. Perspectives on novel therapeutic strategies for right heart failure in pulmonary arterial hypertension: lessons from the left heart. Eur Respir Rev 19: 72–82, 2010.
26. Hines R. Right ventricular function and failure: a review. Yale J Biol Med 64: 295–307, 1991.
27. Jain M, Rivera S, Monclus EA, Synenki L, Zirk A, Eisenbart J, Feghali-Bostwick C, Mutlu GM, Budinger GR, and Chandel NS. Mitochondrial reactive oxygen species regulate transforming growth factor-$\beta$ signaling. J Biol Chem 288: 770–777, 2013.
28. Kasal DA, Neves MF, Oigman W, and Mandarim-de-Lacerda CA. Allopurinol attenuates L-NAME induced cardiomyopathy comparable to blockade of angiotensin receptor. Histol Histopathol 23: 1241–1248, 2008.
29. Kevin LG and Barnard M. Right ventricular failure. Contin Educ Anaesth Crit Care Pain 7: 89–94, 2007.
30. Kumar S, Prahalathan P, and Raja B. Syringic acid ameliorates (L)-NAME-induced hypertension by reducing oxidative stress. Naunyn Schmiedebergs Arch Pharmacol 385: 1175–1184, 2012.
31. Lijnen PJ, Petrov VV, and Fagard RH. Induction of cardiac fibrosis by transforming growth factor-beta(1). Mol Genet Metab 71: 418–435, 2000.
32. Livak KJ and Schmittgen TD. Analysis of relative gene expression data using real-time quantitative PCR and the 2(-delta delta C(T)). Methods 25: 402–408, 2001.
33. Lloyd MH and Wolfensohn SE. *Practical Use of Distress Scoring Systems in the Application of Humane Endpoints. Humane Endpoints in Animal Experiments for Biomedical Research*. London: Royal Society of Medicine Press, 1999, pp. 48–53.
34. Markel TA, Wairiuko GM, Lahm T, Crisostomo PR, Wang M, Herring CM, and Meldrum DR. The right heart and its distinct mechanisms of development, function, and failure. J Surg Res 146: 304–313, 2008.
35. Mehta SR, Eikelboom JW, Natarajan MK, Diaz R, Yi C, Gibbons RJ, and Yusuf S. Impact of right ventricular involvement on mortality and morbidity in patients with inferior myocardial infarction. J Am Coll Cardiol 37: 37–43, 2001.
36. Misík V, Mak IT, Stafford RE, and Weglicki WB. Reactions of captopril and epicaptopril with transition metal ions and hydroxyl radicals: an EPR spectroscopy study. Free Radic Biol Med 15: 611–619, 1993.
37. Nazarewicz RR, Bikineyeva A, and Dikalov SI. Rapid and specific measurements of superoxide using fluorescence spectroscopy. J Biomol Screen 18: 498–503, 2013.
38. Nediani C, Borchi E, Giordano C, Baruzzo S, Ponziani V, Sebastiani M, Nassi P, Mugelli A, d'Amati G, and Cerbai E. NADPH oxidase-dependent redox signaling in human heart failure: relationship between the left and right ventricle. J Mol Cell Cardiol 42: 826–834, 2007.
39. Pacher P, Beckman JS, and Liaudet L. Nitric oxide and peroxynitrite in health and disease. Physiol Rev 87: 315–424, 2007.
40. Queliconi BB, Wojtovich AP, Nadtochiy SM, Kowaltowski AJ, and Brookes PS. Redox regulation of the mitochondrial K(ATP) channel in cardioprotection. Biochim Biophys Acta 1813: 1309–1315, 2011.
41. Schreckenberg R, Maier T, and Schlüter KD. Post-conditioning restores pre-ischaemic receptor coupling in rat isolated hearts. Br J Pharmacol 156: 901–908, 2009.
42. Schreckenberg R, Wenzel S, da Costa Rebelo RM, Röthig A, Meyer R, and Schlüter KD. Cell-specific effects of nitric oxide deficiency on parathyroid hormone-related peptide (PTHrP) responsiveness and PTH1 receptor expression in cardiovascular cells. Endocrinology 150: 3735–3741, 2009.
43. Sekiguchi F, Yamamoto K, Matsuda K, Kawata K, Negishi M, Shinomiya K, Shimamur K, and Sunano S. Endothelium-dependent relaxation in pulmonary arteries of L-NAME-treated Wistar and stroke-prone spontaneously hypertensive rats. J Smooth Muscle Res 38: 131–144, 2002.
44. Shen X, Zheng S, Metreveli NS, and Epstein PN. Protection of cardiac mitochondria by overexpression of MnSOD reduces diabetic cardiomyopathy. Diabetes 55: 798–805, 2006.
45. Soetkamp D, Nguyen TT, Menazza S, Hirschhäuser C, Hendgen-Cotta UB, Rassaf T, Schlüter KD, Boengler K, Murphy E, and Schulz R. S-nitrosation of mitochondrial connexin 43 regulates mitochondrial function. Basic Res Cardiol 109: 433, 2014.
46. Suda O, Tsutsui M, Morishita T, Tanimoto A, Horiuchi M, Tasaki H, Huang PL, Sasaguri Y, Yanagihara N, and Nakashima Y. Long-term treatment with Nw-nitro-l-arginine methyl ester causes arteriosclerotic coronary lesions in endothelial nitric oxide synthase-deficient mice. Circulation 106: 1729–1735, 2002.
47. Tastan I, Schreckenberg R, Mufti S, Abdallah Y, Piper HM, and Schlüter KD. Parathyroid hormone improves contractile performance of adult rat ventricular cardiomyocytes at low concentrations in a non-acute way. Cardiovasc Res 82: 77–83, 2009.
48. Tessari P, Cecchet D, Cosma A, Vettore M, Coracina A, Millioni R, Iori E, Puricelli L, Avogaro A, and Vedovato M. Nitric oxide synthesis is reduced in subjects with type 2 diabetes and nephropathy. Diabetes 59: 2152–2159, 2010.
49. Verzi MP, McCulley DJ, De Val S, Dodou E, and Black BL. The right ventricle, outflow tract, and ventricular septum comprise a restricted expression domain within the secondary/anterior heart field. Dev Biol 287: 134–145, 2005.
50. Voelkel NF, Quaife RA, Leinwand LA, Barst RJ, McGoon MD, Meldrum DR, Dupuis J, Long CS, Rubin LJ, Smart FW, Suzuki YJ, Gladwin M, Denholm EM, Gail DB; National Heart, Lung, and Blood Institute Working Group on Cellular and Molecular Mechanisms of Right Heart Failure. Right ventricular function and failure: report of a National Heart, Lung, and Blood Institute working group on cellular and molecular mechanisms of right heart failure. Circulation 114: 1883–1891, 2006.

51. Zaffran S, Kelly RG, Meilhac SM, Buckingham ME, and Brown NA. Right ventricular myocardium derives from the anterior heart field. Circ Res 95: 261–268, 2004.

Address correspondence to:
*Dr. Rolf Schreckenberg*
*Physiologisches Institut*
*Justus-Liebig-Universität Gießen*
*Aulweg 129*
*Gießen D-35392*
*Germany*

*E-mail:* rolf.schreckenberg@physiologie.med.uni-giessen.de

Date of first submission to ARS Central, September 30, 2014; date of final revised submission, April 24, 2015; date of acceptance, May 13, 2015.

**Abbreviations Used**

ACE = angiotensin-converting enzyme
Act-D = actinomycin D
ANP = atrial natriuretic peptide
BNP = brain natriuretic peptide
bpm = beats per minute
BW = body weight
C = control group
Chx = cyclohexemide
DCB = disulphide cross-bridges
DHE = dihydroethidium
$eNOS^{-/-}$ = homozygous eNOS knockout
Gclc = glutamate-cysteine ligase, catalytic subunit
GOT/GPT = glutamate-oxaloacetate transaminase/glutamate-pyruvate transaminase
Gpx1 = glutathione peroxidase 1
$H_2O_2$ = hydrogen peroxide
HADHA = hydroxyacyl-CoA dehydrogenase, alpha subunit
HPRT = hypoxanthine-guanine phosphoribosyltransferase
HRP = horseradish peroxidase
L = L-NAME group
LC = L-NAME/captopril group
LT = L-NAME/tempol group
LV = left ventricle
LVDP = left ventricular developed pressure
LW = liver wet weight
MHC-$\alpha$ = myosin heavy chain alpha
MHC-$\beta$ = myosin heavy chain beta
NO = nitric oxide
NOX2 = cytochrome b-245 heavy chain
Nrf(-1,-2) = nuclear respiratory factor (-1, -2)
$ONOO^-$ = peroxynitrite
oxTm = oxidized tropomyosin
P22phox = cytochrome b-245 light chain
PGC-1$\alpha$ = peroxisome proliferator-activated receptor gamma coactivator 1-alpha
RAAS = renin-angiotensin-aldosterone system
ROS = reactive oxygen species
RT-PCR = reverse transcription polymerase chain reaction
RV = right ventricle
RVEDP = right ventricular end-diastolic pressure
RVSP = right ventricular systolic pressure
SHR = spontaneously hypertensive rats
SOD (1-3) = superoxide dismutase (1-3)
TGF-beta1 = transforming growth factor beta1
Tm = tropomyosin
TXNRD1 = thioredoxin reductase 1
UCP(-2,-3) = mitochondrial uncoupling protein (-2, -3)